Volume I

LLE
REVIEW

September - November 1979

UR
LLE

EDITOR'S NOTE

This is the first in a series of quarterly reviews of the activities and accomplishments of the Laboratory for Laser Energetics at the University of Rochester. The principle activity at LLE is inertial confinement fusion research with high power neodymium glass lasers (λ = 1.054 μm). Research in a few areas unrelated to ICF is also being pursued at LLE and will occasionally be included in these reviews. In addition, the laser systems at LLE make up the National Laser Users Facility. It is expected that in the near future outside users will be involved in a wide variety of research studies at LLE, which will also be reviewed when appropriate.

IN BRIEF

Recent implosion experiments carried out with the ZETA six beam laser system have yielded substantially higher compressed densities than earlier exploding pusher experiments. By utilizing thicker target walls, compressed DT densities of up to 2 g/cm^3 (10x liquid density) and fuel $\rho R = 1.4 \times 10^{-3}$ g/cm^2 have been inferred from x-ray imaging. Compressed Argon densities of 6 g/cm^3 and $\rho R = 1.5 \times 10^{-3}$ g/cm^2 have been measured with spectral line broadening methods. The high Argon densities are attributed in part to radiational cooling during the implosion.

LLE REVIEW
Volume I

Editor: E. I. Thorsos (716-275-5164)

Contents: September - November 1979

LASER SYSTEMS REPORT

A cutaway view of the Laboratory for Laser Energetics at the University of Rochester is shown in Figure 1a, and the laser systems of the National Laser Users Facility at LLE are indicated in Figure 1b. The 24 beam, 12 TW OMEGA Laser System is nearing completion and is in the large laser bay at the rear of the building in Figure 1 with the OMEGA target chamber assembly to the left. The 3TW ZETA laser system is operational and is composed of 6 of the OMEGA laser beams. The single beam Glass Development Laser is also operational and, with reference to Figure 1, is located on the lower level.
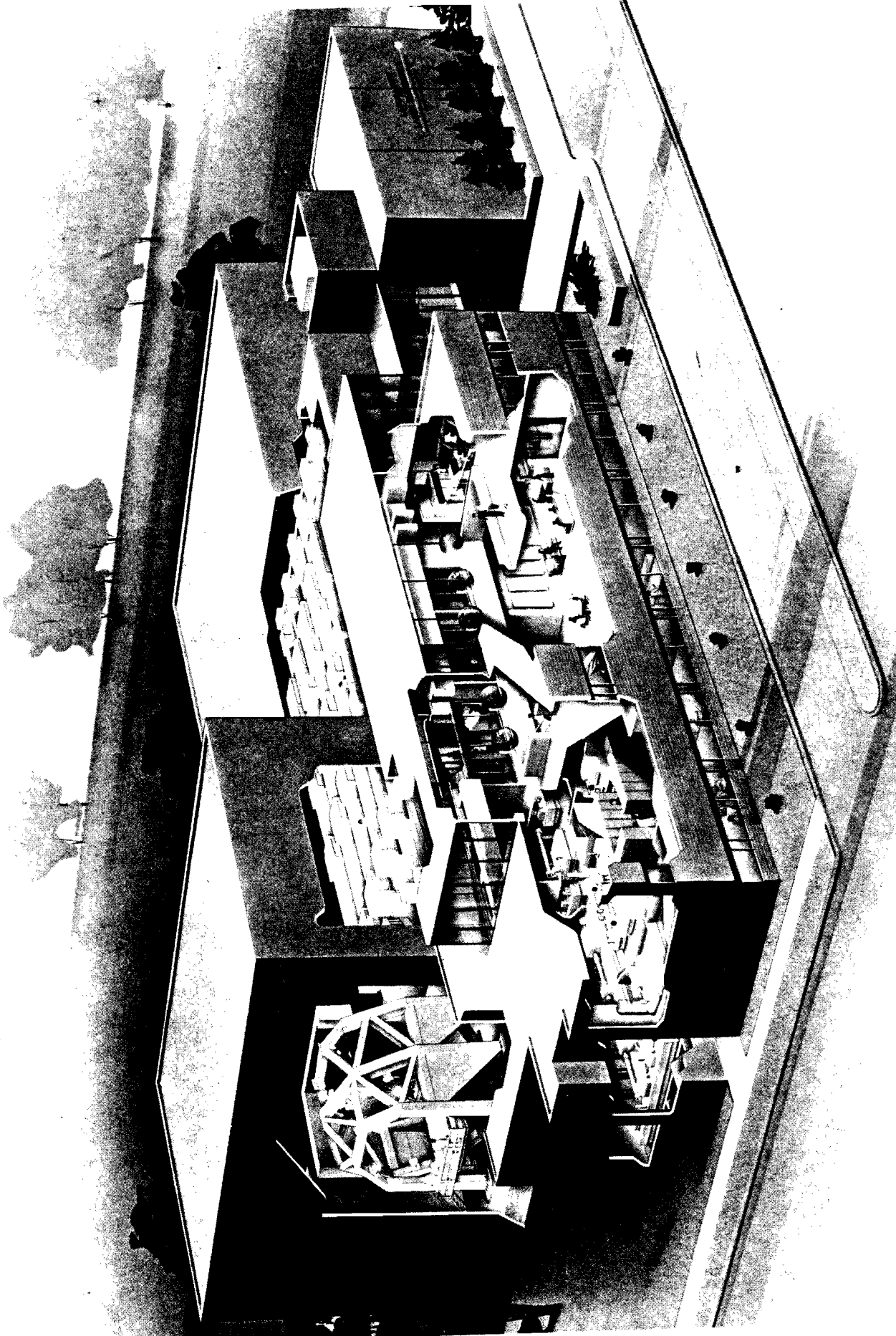
Figure 1a The Laboratory for Laser Energetics at the University of Rochester

University of Rochester
Laboratory for Laser Energetics

OMEGA TARGET LABORATORY

OMEGA (24 BEAM) LASER LABORATORY

OMEGA AMPLIFIER-CAPACITOR BAY

LASER COMPUTER FACILITY (LCF)

OMEGA MAIN CONTROL ROOM

OMEGA DIAGNOSTIC CONTROL ROOM

ACTIVE MIRROR LABORATORY

X-RAY TARGET INTERACTION LABORATORY

GDL CONTROL ROOM

GDL TARGET LABORATORY

GLASS DEVELOPMENT LASER LABORATORY (GDL)
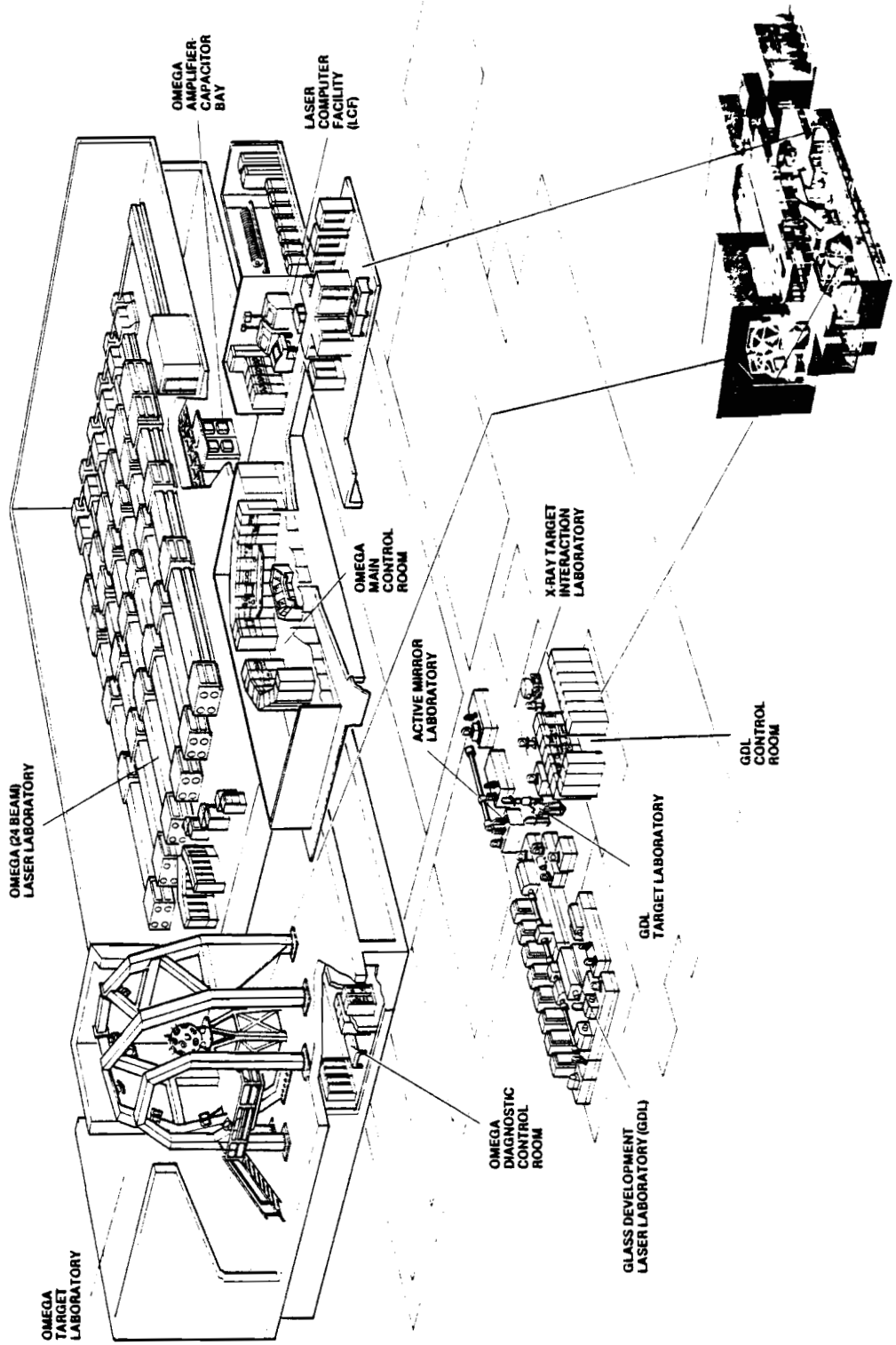
Figure 1b   The laser systems at the National Laser Users Facility at LLE

ZETA Laser System

The ZETA laser system is composed of the first 6 of the 24 OMEGA laser beam lines. A separate ZETA target chamber has been utilized for symmetrical illumination target experiments beginning in October 1978. A total of 110 taret shots were executed on ZETA in the period from September 1 to November 7, 1979. A weekly log of ZETA target shots for all of 1979 is shown in Figure 2. During weeks 40-42, the wall separating the ZETA beams and the remaining 18 was taken down. The ZETA components were then cleaned and completely realigned. ZETA target experiments were temporarily suspended on November 7 in order to concentrate the efforts of the Engineering Division and the Operations

ZETA TARGET SHOTS FOR 1979
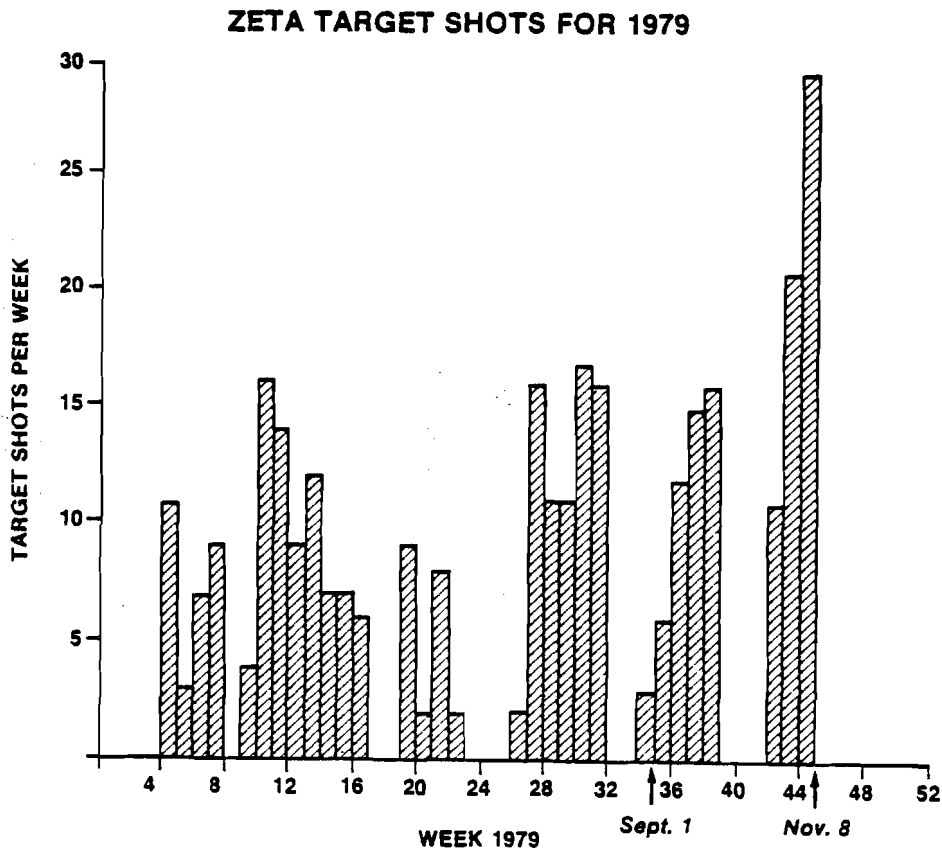
Figure 2

Group on the activation of the remaining 18 OMEGA beam lines. In the future, the 6 ZETA beam lines will serve a dual role as part of the full OMEGA 24 beam system, and when directed to the ZETA experimental area, as the ZETA laser system. This will allow the ZETA experimental program to continue indefinitely while the OMEGA experimental facility is developed.

For the target shots in this reporting period, the ZETA laser output was in the energy range of 50-150 J in 50-70 psec pulses. 50 shots were devoted to thin wall ($\sim$ 1 μm) exploding pusher experiments. 52 shots were carried out on targets with thick walls (up to 10 μm) in order to obtain high compressed densities; these targets were filled with DT, D_2, or Argon. In addition 8 target shots were utilized for diagnostic and laser system checkout. For these experiments, the beams were balanced in energy by an amount that varied from ±6% to ±15% and the arrival times of the beams on target were within 3-4 psec. Further details on the experimental results are given in Progress In Laser Fusion.

OMEGA Laser System

Progress has continued in the last quarter on the assembly and activation of the remaining 18 of the 24 OMEGA Laser System beam lines. This activity will culminate in the DOE laser performance test presently scheduled for mid January, 1980. The following milestones have been achieved:

1. All laser beamline hardware is now installed and aligned up to and including the end mirrors and beam diagnostic packages (Figure 3).

2. Two four beam clusters have been fully tested for gain, and have had high power beams propagated through them. All clusters are to be fully gain tested and characterized by January 1, 1980.

3. The target area structures and the primary personnel platform are now complete with the exception of final painting (Figure 4). A contract has also been let for a secondary personnel platform.

4. The first production assemblies of both the OMEGA focus lens mount and final turning mirror mount have been received and tested.

The OMEGA target chamber is now scheduled for delivery by February 1, 1980.
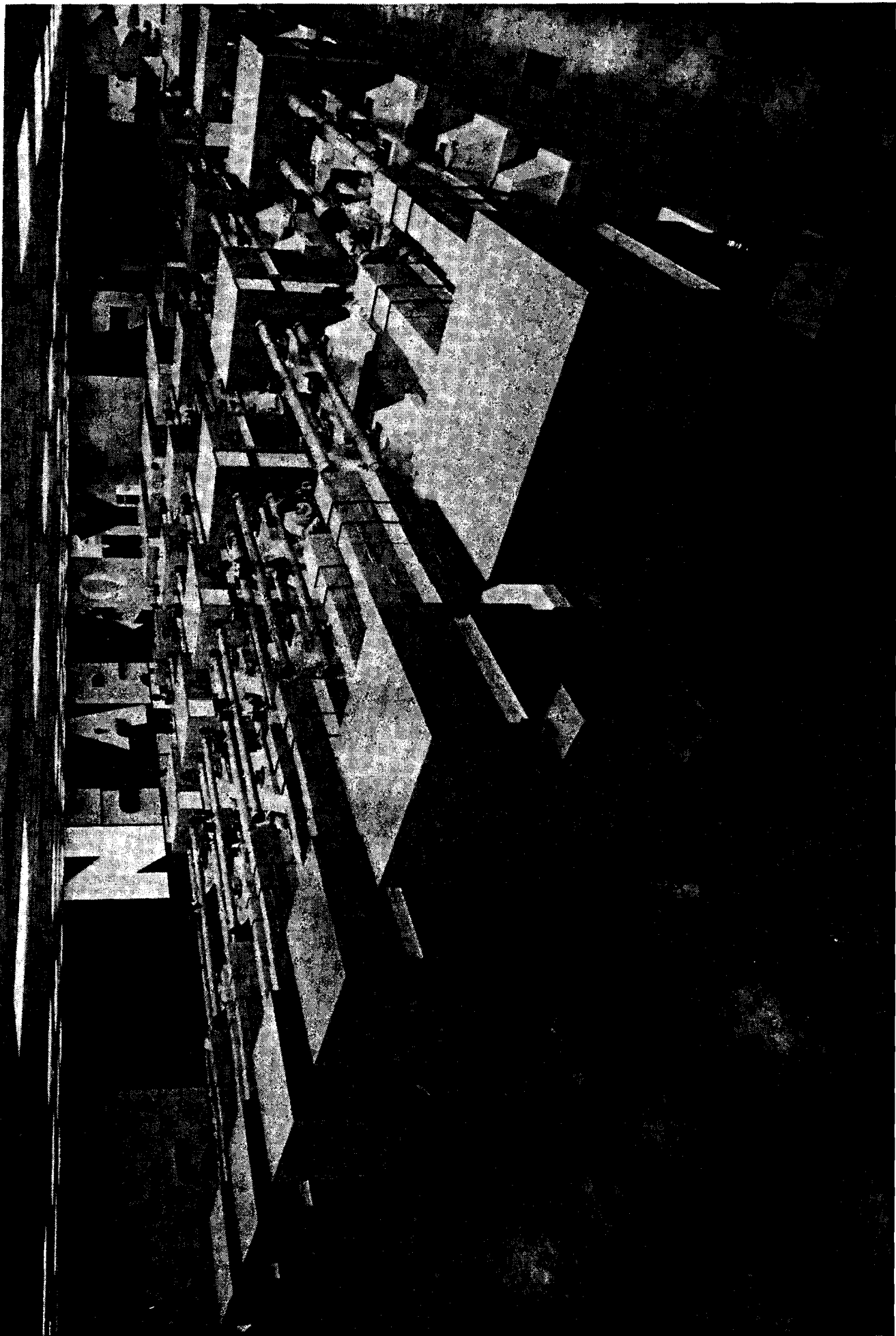
Figure 3   OMEGA laser bay 10/79
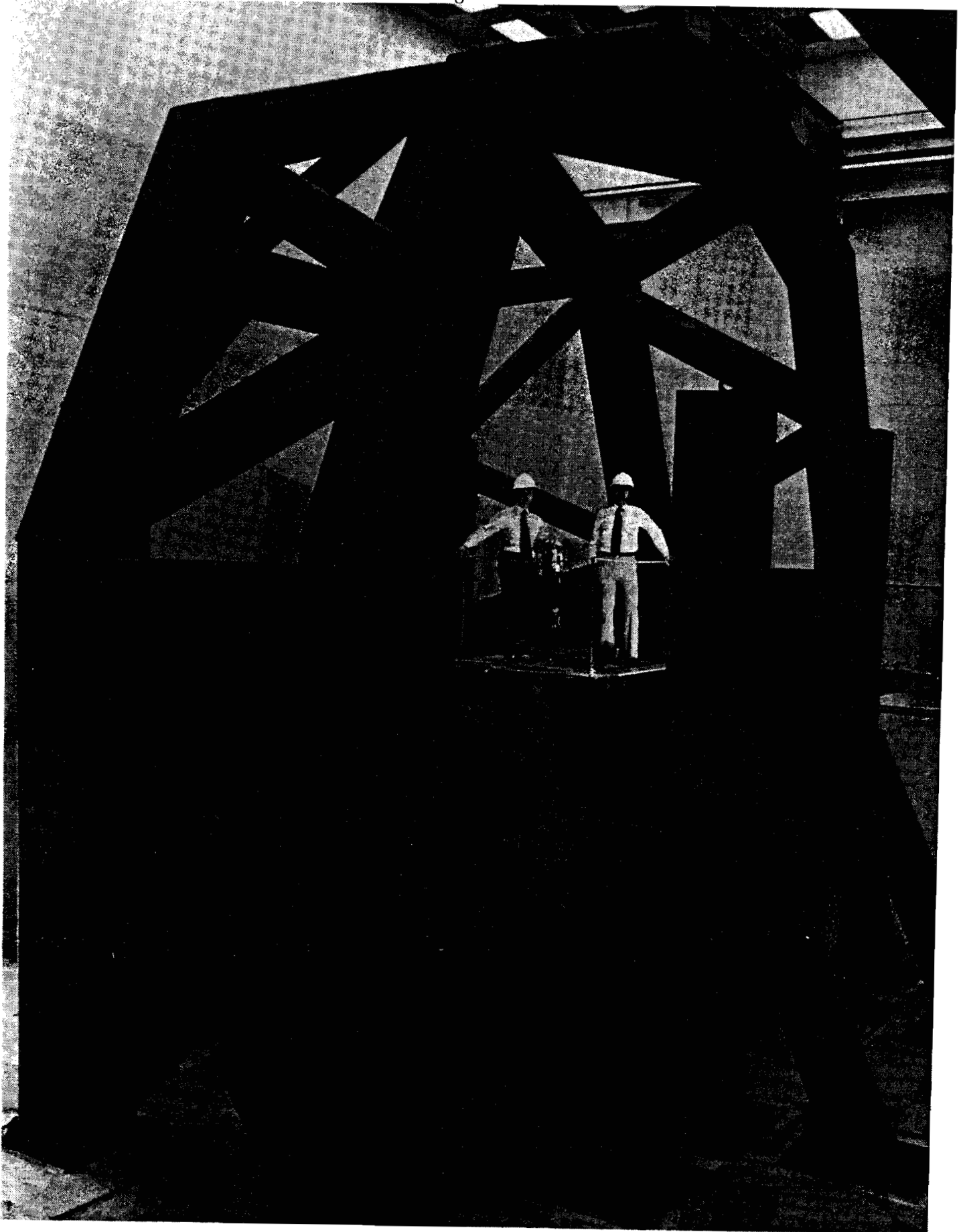
Figure 4   OMEGA target structure (9/79) before construction of primary
personnel platform

Glass Development Laser (GDL)

The original OMEGA beam line prototype, which is comparable in laser performance to a single OMEGA beam line, has been utilized for a wide variety of target experiments since early 1978. The GDL beam can be directed into two separate laser plasma experimental areas or into the OMEGA Booster Program experimental area for active mirror studies. The beam can also be split into two beams for implosion experiments.

During the period September 1, 1979 through November 30, 1979, a total of 298 shots were taken on GDL for a variety of experiments.

1. INTERACTION EXPERIMENTS: A total of 78 shots were taken in support of research in the areas of fast ion production and high energy suprathermal electron generation.

2. TRANSPORT EXPERIMENT: 30 shots were for a preliminary phase of a joint SANDIA-LLE-KMS experiment. These shots examined the burn through of thin (1-3μm) plastic layers at incident laser intensities of $10^{13} - 10^{14}$ W/cm^2. Charge states of blow-off ions were analyzed (with a Thomson parabola) to determine when the boron substrate was heated significantly.

3. X-RAY GROUP: 32 shots were taken to support x-ray laser experiments, applications of laser produced x-rays in biophysics, and diagnostic development.

4. SHORT WAVELENGTH CONVERSION PROGRAM: 26 shots were used for efficiency and birefringence studies of laser frequency doubling with Type II KDP crystals.

5. DAMAGE TESTING: A total of 125 shots were taken in support of coating damage measurements in the damage test facility.

6. SURFACE ANNEALING BY LASER IRRADIATION: 7 shots were conducted for an outside user (Bell Laboratories) measuring the effects of high power laser irradiation on semiconductor materials.

PROGRESS IN LASER FUSION

Exploding Pusher Experiments on ZETA

An extensive series of implosion experiments utilizing DT filled glass microballoon targets with thin walls (0.6 - 1.4 μm) has been carried out on the ZETA laser system during 1979. The symmetrical illumination provided by the 6 ZETA beams has produced impressive results in terms of implosion symmetry and neutron yield for these exploding pusher implosions. A neutron yield of 1.5 x 10^9 was obtained for 1.67 TW of laser power (on target) in a 72 psec pulse, a record yield for this power level. Some of the important results of these experiments will be reviewed in this section.

Figure 5 is an example of an x-ray image (2-3 keV x-ray energy) showing the implosion symmetry routinely obtained. The diameter of the DT fill is typically reduced by a factor of 3-4 during these implosions. This observation, together with the initial DT density of ~ 4 mg/cm^3, clearly shows that exploding pusher implosions compress DT to roughly liquid density (0.2 g/cm^3).

Neutron yields from a number of exploding pusher implosions are shown as a function of specific absorbed energy in Figure 6. For all these experiments, the ZETA beams were focused about 2 radii behind the target center, which results in symmetry similar to Figure 5. The attainment of yields greater than 10^9 for less than 2 TW of laser power

is attributed to the high degree of implosion uniformity obtained with the ZETA laser system.

EXPLODING PUSHER IMPLOSION
DT Compressed to ~Liquid Density

|————— Initial Diameter —————|
111 μm
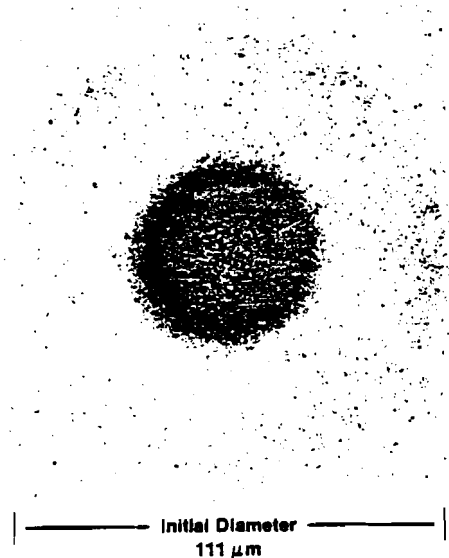
Shot 2452
Wall: 1.23 μm SiO₂
Fill: 4.2 mg/cm³ DT (20 atm)
Laser: 1.66TW, 60 psec

Figure 5   X-ray image of ZETA implosion

The solid line in Figure 6 was obtained by fitting the data with a very simple model, which assumes that the neutron yield can be considered only a function of DT ion temperature for these experiments, e.g., the slow dependence of compression on specific absorbed energy is ignored. The DT ion temperature, T_i, is taken as proportional to the specific absorbed energy, ε. The neutron yield $Y \sim n_D n_T V \tau \langle \sigma v \rangle$, where the disassembly time τ is proportional to the (ion sound speed)$^{-1}$ or to $T_i^{-1/2}$, and where the velocity averaged DT reaction cross section $\langle \sigma v \rangle \sim T_i^{-2/3} \exp(-19/T_i^{1/3})$ with T_i in keV. Thus $Y = A\varepsilon^{-7/6} \exp(-B/\varepsilon^{1/3})$.

NEUTRON YIELD VERSUS SPECIFIC ABSORBED ENERGY
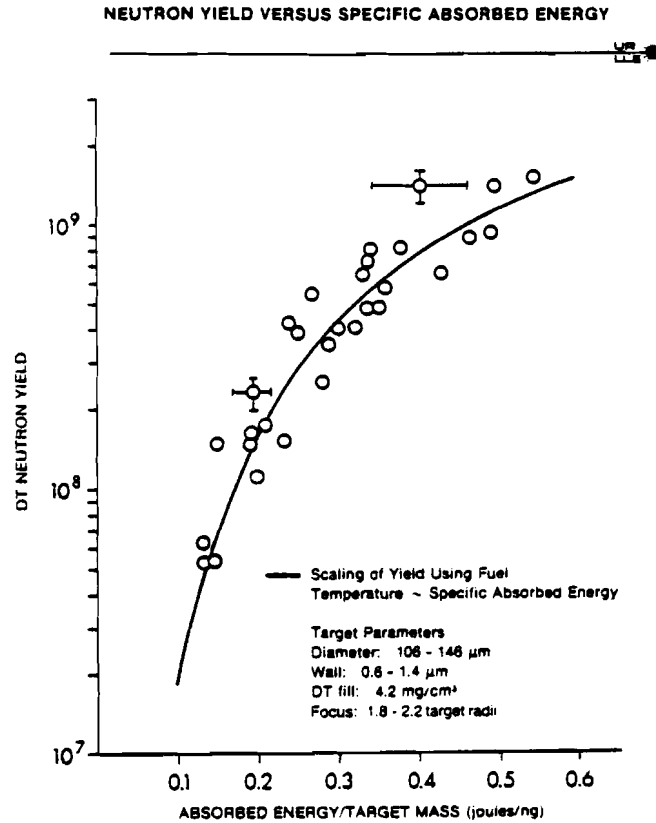
Figure 6

The constants A and B are chosen to give the best curve fit through the data. In the model the rolloff in the yield curve as ε increases is chiefly a result of the temperature dependence of $<\sigma v>$. A major challenge for the future will be to move above this scaling by increasing the compressed DT density.

The 1-D Lagrangian hydrodynamic implosion code LILAC (including multi- group suprathermal electron transport) has been utilized to simulate these experiments. The computations generally support the features of the simple model above and the computed yield is quite close to experiment, generally higher than experiment by a factor of

14

1-2. Since these computations are performed with no artificial reduction in the yield calculation to account for implosion asymmetries, for example, the reasonable agreement is another indication of good spherical symmetry for these experiments.

An examination of the effect of beam focusing on neutron yield is shown in Figure 7. In this figure the measured/calculated neutron yield is plotted versus the beam focal position. The calculated yield was taken from the simple scaling model of Figure 6 and is used to remove the dependence on specific absorbed energy. For beam focusing near 2 radii, the yield ratio scatters about 1.0, since the scaling

**COMPARISON OF MEASURED AND PREDICTED* NEUTRON YIELD
AS A FUNCTION OF BEAM FOCUS POSITION**
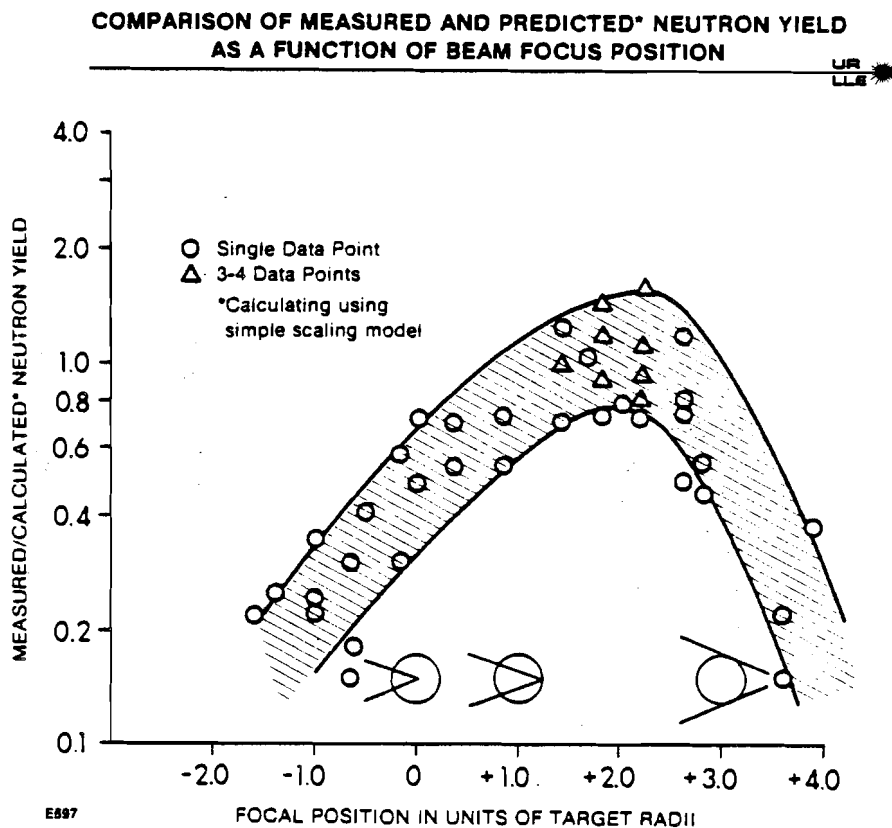
Figure 7

model was normalized at that focal position. This focusing position is optimum for neutron yield. As the focal position is shifted to surface focus (focal position of -1 in Figure 7) the neutron yield drops dramatically relative to the scaling model. The x-ray imaging results[1] also show a steady increase in structure as the focal position is shifted from +2 to -1, implying that only sections of the target are being imploded at high velocity when the beams are focused on the surface. The decrease in neutron yield would appear to result from the decrease in implosion symmetry.[2] The decrease in relative yield for focal positions beyond +2 is not clearly understood.

Alpha particle and proton energy spectra have also been measured for these experiments with a quadrupole time-of-flight detector. From the width of the alpha spectrum, DT ion temperatures have been measured from 2 to 6 keV and to be approximately proportional to the specific absorbed energy, as assumed in the simple neutron scaling model above. The mean alpha energy can be expected to be downshifted during passage through the glass tamper by an amount which depends on the temperature and ρR of the tamper. Energy downshifts have been observed, but for high specific absorbed energy implosions, alpha energy upshifts are seen instead[3] (Figure 8). This is interpreted as acceleration of the alpha particles as they traverse an electrostatic potential generated by suprathermal electrons. Such a potential would be expected from high energy electrons which escape the target entirely and from quasi-neutral and sheath potentials in the corona. For the data of Figure 8, a minimum estimate for the potential of up to 215 kV can be deduced from the magnitude of the energy upshift

SCALING OF ALPHA PARTICLE MEAN
ENERGY WITH SPECIFIC ABSORBED ENERGY
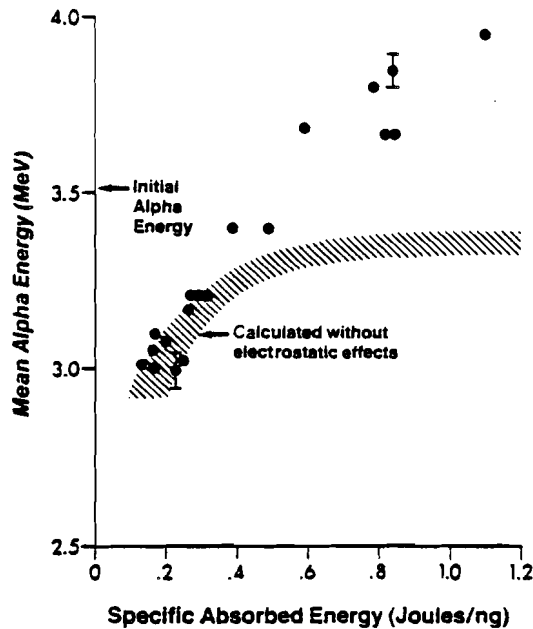
Figure 8

alone. By comparing with LILAC calculations of the expected alpha spectrum without electrostatic effects (hatched region, Figure 8), time averaged potentials up to 300 kV can be inferred.

In order to clarify the specific absorbed energy dependence of the alpha energy upshift, Figure 9 gives the LILAC result for the time history of the cummulative alpha particle production relative to the laser pulse for low and high specific absorbed energy shots. For the low specific absorbed energy shot 1917 the implosion velocity is relatively low and the alpha particles are produced essentially after the laser pulse. For shot 1917 and similar shots, alpha particle energy downshifts are observed. For shot 1801, with higher specific absorbed energy, the shorter implosion time results in alpha particle

ALPHA PRODUCTION·TIME HISTORY CALCULATION
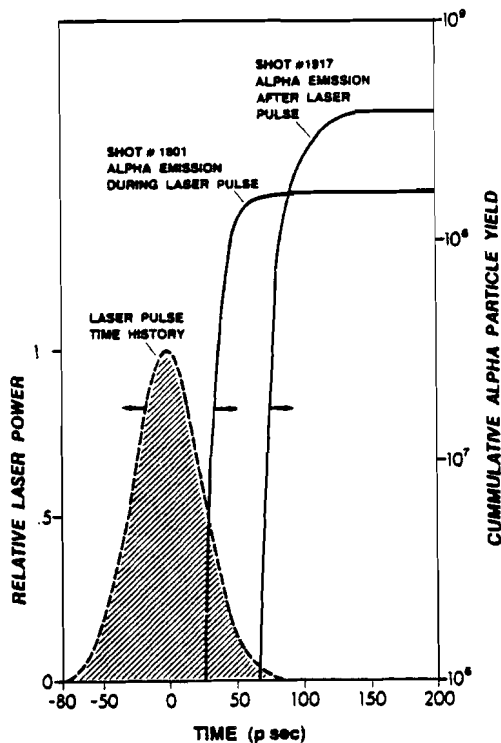
Figure 9   Alpha production time history relative to the laser pulse
calculated by the code LILAC: high specific absorbed energy
(0.79 J/ng) for shot 1801; low specific absorbed energy
(0.26 J/ng) for shot 1917

production during the laser pulse. For shot 1801 and similar shots,
alpha particle energy upshifts are observed. This is consistant with
an electrostatic potential which decays rapidly after the laser pulse
and hence after cessation of energetic electron production. Rapid
potential decay may occur through neutralizing currents from the target
stalk or through cooling of the energetic electrons by expansion and
fast ion production. It should be noted that for cases with alpha
energy upshifts, the time varying nature of the electrostatic potential
can also broaden the spectrum substantially, thereby complicating DT
ion temperature determinations for such cases.

Finally, the fractional absorption of incident 1.054 μm laser radiation onto targets in 50-70 psec pulses has been measured with an array of 12 differential plasma calorimeters. The results for absorption versus beam focal position are shown in Figure 10. The absorption fraction is typically 30% at a focal position of 2 radii behind target center, the optimum position for neutron yield. The peak intensity for this case is about 5×10^{15} W/cm^2. Near surface focus, the absorption fraction rises to 50%, while implosion symmetry and yield are substantially degraded. For surface focus, the peak intensity is $\geq 10^{17}$ W/cm^2.

In an attempt to understand the absorption mechanism in the varying focusing regions, we have employed an axially symmetric ray

ABSORPTION AS FUNCTION OF FOCUSING
Zeta 6-Beam, 3TW, Symmetrical Irradiation Facility

FOCUSING IN TARGET RADII
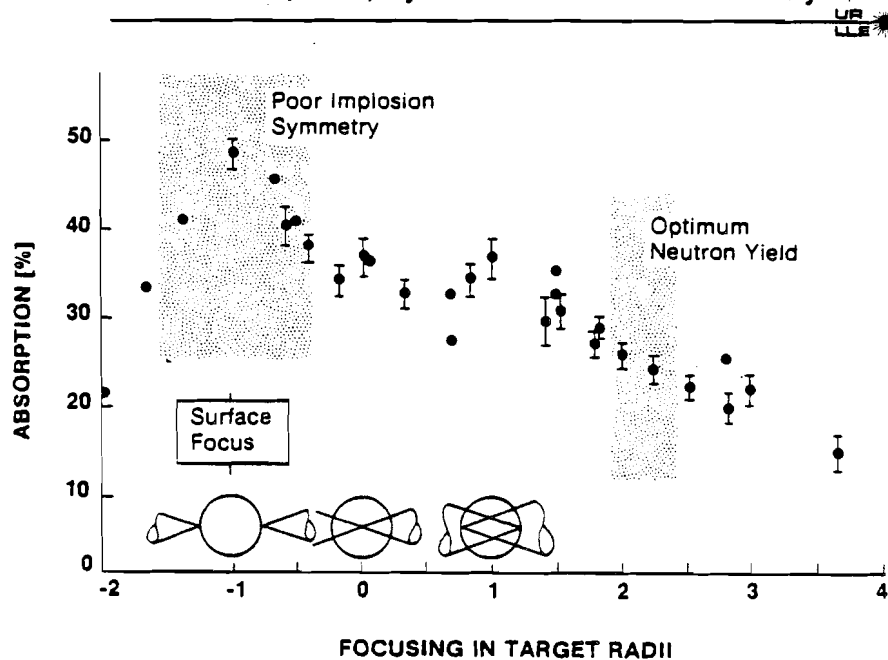
E708

Figure 10

tracing code to compute resonance absorption for circularly polarized beams taking into account profile steepening and incident angle variations across the beam profile. A comparison of the calculated and experimental absorption is shown in Figure 11. We observe that this resonance absorption model can account for the experimental data beyond a focal position of 2 target radii. On the other hand, there is substantial disagreement for other focusing conditions where the intensity increases to the $10^{16} - 10^{17}$ W/cm^2 range, and where strong spatial modulation of the incident intensity exists because of low irradiance conditions between the beams. It can only be speculated at this point that effects such as deformation of the critical density surface may be essential for calculation of absorption in this regime.

ABSORPTION VERSUS FOCUS

FOCUSING IN TARGET RADII
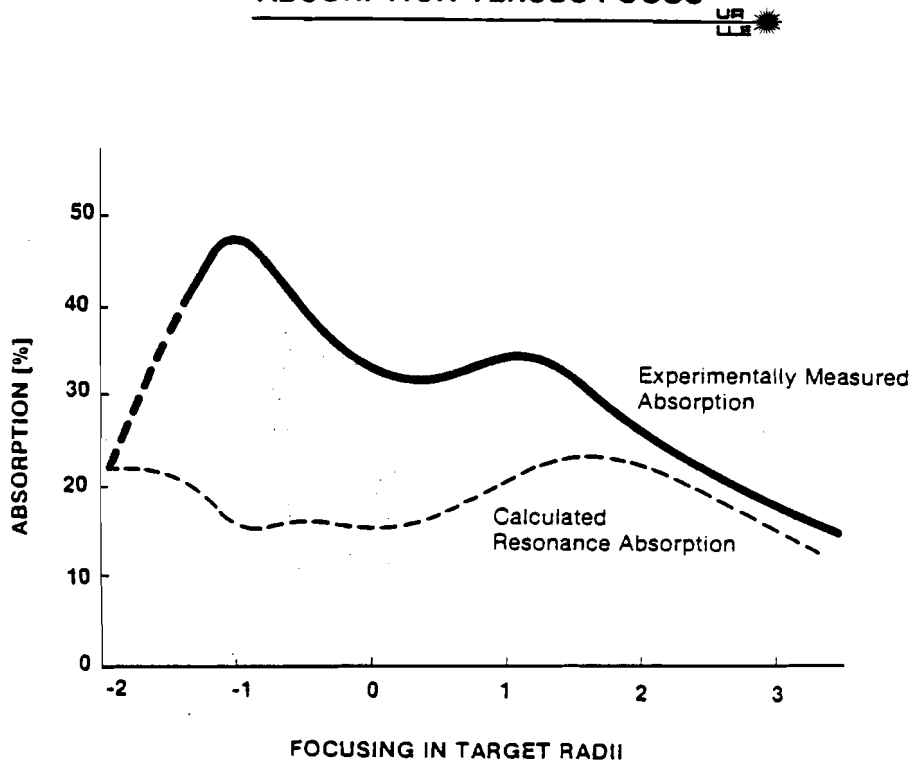
E710

Figure 11

1. E. I. Thorsos, T. C. Bristow, J. A. Delettrez, J.M. Soures, and J. E. Rizzo, Appl. Phys. Lett. <u>35</u>, 598 (1979).

2. It is probable that a higher percentage of the absorbed energy appears in fast ions as the intensity increases near surface focus. This will also have the effect of decreasing the yield.

3. Y. Gazit, J. Delettrez, T. C. Bristow, A. Entenberg, and J. Soures, Phys. Rev. Lett. <u>43</u>, 1943 (1979).

Intermediate Density Experiments on ZETA: DT Fill

In order to obtain compressed DT densities higher than liquid density, a number of experiments have been performed with DT filled plastic coated glass microballoon targets with plastic thicknesses up to 10 μm. Up to 150 J of laser energy was applied in 50-80 psec pulses to targets with diameters ranging from 80-130 μm. Compressed DT densities up to 10x liquid density have been inferred with x-ray imaging for these implosion experiments.

X-ray pinhole camera imaging has shown in exploding pusher implosions that the ZETA laser system is capable of producing symmetric implosions when the beams are focused several radii behind the target. This observation has been extended to higher compression implosions (up to a compression of ~ 500) with thick shell targets. To clearly resolve the "inner ring," that is, the inside of the SiO_2 tamper location, requires imaging with relatively hard x-rays to avoid opacity effects from the surrounding cold tamper. The hardest x-ray channel in the x-ray pinhole camera is in the 3-4 keV range. This x-ray energy coupled with 3-4 μm diameter pinholes yields quite good resolution (~ 4 μm) as shown in Figure 12 (inset). The densitometer scan shows for this implosion that the SiO_2 stagnated with an inner diameter of 20 μm. The DT inside radiates negligibly because of its lower Z. Assuming the fill gas is entirely trapped, this diameter immediately yields a compressed density. There are pitfalls associated with this method, however. To be convincing, the following conditions should be met: (1) the focusing of the laser beams should be optimized for symmetric
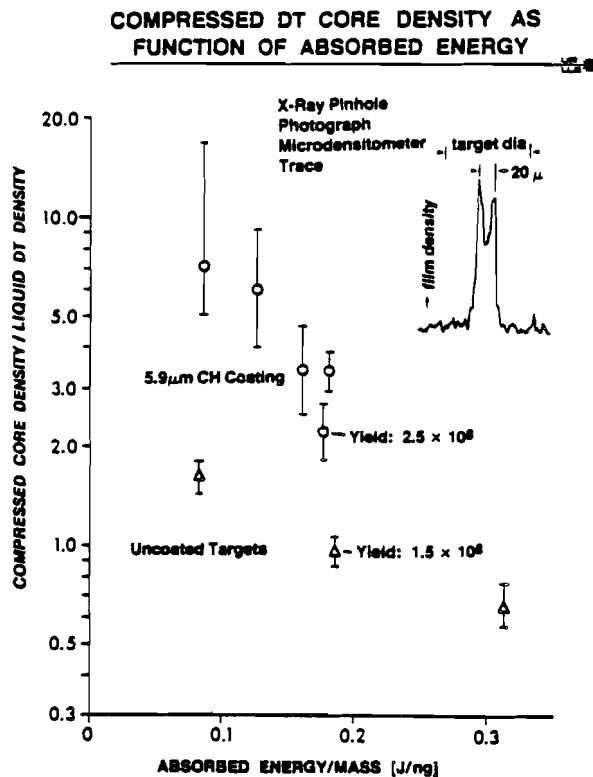
Figure 12

implosions; (2) the inner ring should be nearly spherically symmetric, as observed with more than one view of the implosion, and (3) the compression results should form a smooth and consistent trend to higher densities as the wall thickness is increased. All of these conditions have been met in our experiments; in particular, two pinhole cameras have been used to check on symmetry.

Results for compressed DT densities from x-ray imaging for two kinds of targets are shown in Figure 12. The three triangular points are for relatively thin targets, in this case uncoated glass microballoons filled with 4.2 mg/cm^3 DT. We would expect these targets to behave in typical exploding pusher fashion yielding compressed DT

densities near liquid density, which they do. The other points are for thicker shell targets: 6 μm of CH on top of 0.8 μm of SiO_2 with a total target diameter of about 90 μm. These targets are filled with about 10 mg/cm^3 of DT. The increased shell mass for these targets leads to increased compressed density as would be expected from simple exploding pusher scaling arguments. The rise in compressed density for reduced specific absorbed energy would be expected qualitatively from (1) lower fuel preheat by suprathermal electrons (at lower incident intensity) and from (2) less shock heating in the fuel from the lower implosion velocity resulting in a lower fuel adiabat. This result suggests that in comparing compressed density as a function of target wall thickness, it may be advantageous to hold the specific absorbed energy constant. Figure 13 shows that as the wall thickness is increased holding the

COMPRESSED DT CORE DENSITY
AS FUNCTION OF TARGET THICKNESS
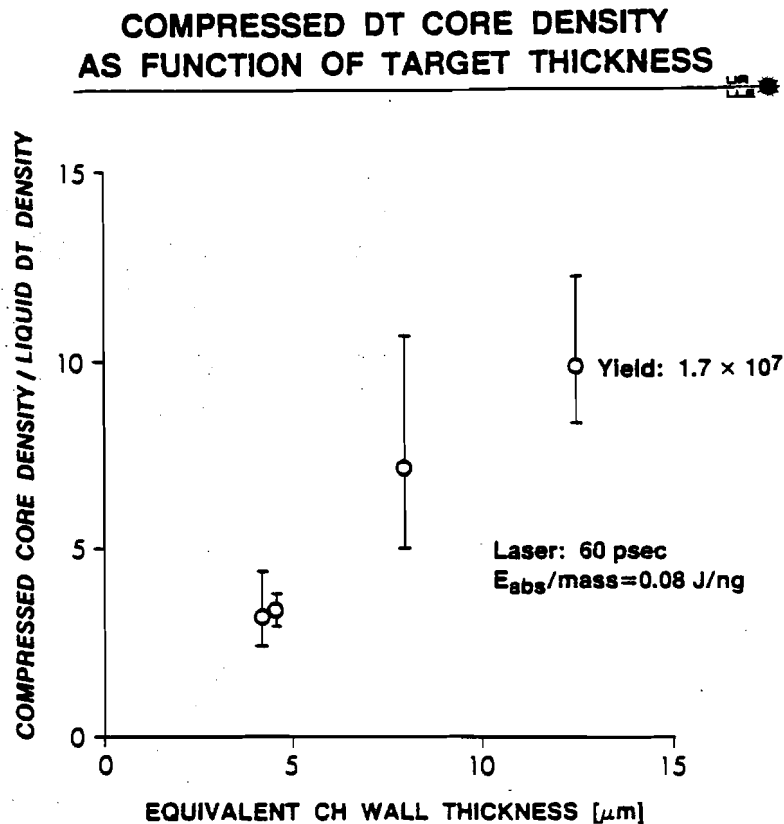
Figure 13

specific absorbed energy constant, the compressed DT density is also increased up to 10x liquid density. The equivalent CH wall thickness is obtained by replacing the SiO_2 by an amount of CH of equal mass.

Implosion times were also obtained for these experiments with an x-ray streak camera. Analysis of this data and overall comparison with LILAC simulations are presently underway.

Intermediate Density Experiments on ZETA: Ar Fill

Argon filled plastic coated glass microballoon targets have also been imploded with short, high intensity, laser pulses: 100 - 150 J in ~ 50 psec laser pulses. The role of the Argon was two-fold: (1) to partly mitigate the effect of preheat through radiational cooling and thereby enable a higher compression, and (2) to serve as a direct diagnostic of the compressed density (ρ) and the quality of confinement (ρR). The measurement of the density (using x-ray line Stark broadening) allows an experimental verification of whether a given predicted compression (with any fill) can actually be achieved or whether it is prevented by the lack of perfect spherical symmetry, instability or shell-fill mixing. The various x-ray lines utilized for density determinations are predicted to have different widths and _very different shapes_, and therefore a consistent agreement with this large number of observables constitutes a highly reliable determination of the compression. Densities in the range of 4-6 g/cm^3 (n_e = 1.0 - 1.5 x 10^{24} cm^{-3}) at temperatures ~1 keV were deduced from the Stark profiles of various Ar^{+16}, Ar^{+17} x-ray lines.[1] These densities are achieved partly due to radiational cooling of the high-Z fill gas and show that symmetric illumination can result in high volume compession (> 1000).

In order to employ the observed lines for ρ and ρR determinations, an estimate is needed for the temperature during the time of emission, and the opacity (self-absorption of the lines). Fortunately, the line profiles are not very sensitive to temperature, especially for helium-like ions. For high density shots T_e was found to be about 0.8

keV using various line intensity ratios. It can be shown on rather general grounds for these experiments that the optical depth of the Ar^{+17} Lyman-β line will be near unity or less, and therefore the line profile will be only modestly affected by opacity. In addition, the Lyman-β profile has a double peak structure, and the peak separation is relatively insensitive to opacity (compared to the width, for example). The Lyman-β peak separation is therefore very useful in obtaining a first estimate of density. An example of a density determination is shown in Figure 14 for shot 3231. The Lyman-β line was fitted with a profile for an electron density $n_e = (1.5 \pm 0.4) \times 10^{24}$ cm^{-3} (which corresponds to $\rho \sim 6$ g/cm^3) without any opacity correction; a small opacity correction would further improve agreement with experiment. Analysis of other lines for this shot gives consistent results.
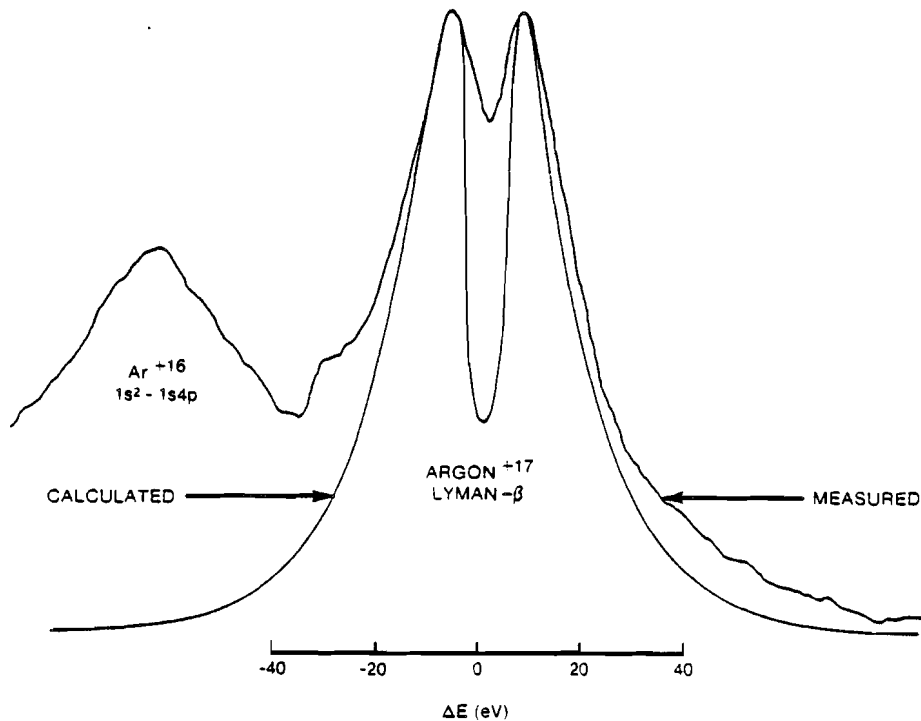
Figure 14 Argon Lyman-β line from shot 3231 with fitted profile. The density determination was $n_e = (1.5+0.4) \times 10^{24}$ cm^{-3} or $\rho \sim 6$ g/cm^3

Some of the more dramatic profile changes with density are shown by the spectral profile of the $1s^2 - 1s3p$ line of Ar^{+16} and its forbidden neighbor $1s^2 - 1s3d$. Figure 15 shows a comparison of the profile of these lines for a high density shot (2495) and for a lower density shot (2416). At high plasma densities the quadratic Stark effect should cause the forbidden line to increase in intensity and the two lines to move apart and broaden. All these features are clearly seen in Figure 15. Stark profile fitting (Figure 16) yields an electron density $n_e = (0.96 \pm 0.24) \times 10^{24}$ cm^{-3} ($\rho \sim 3.8$ g/cm^3).

HIGH DENSITY MEASUREMENT OF IMPLODED ARGON-FILLED MICROBALLOON
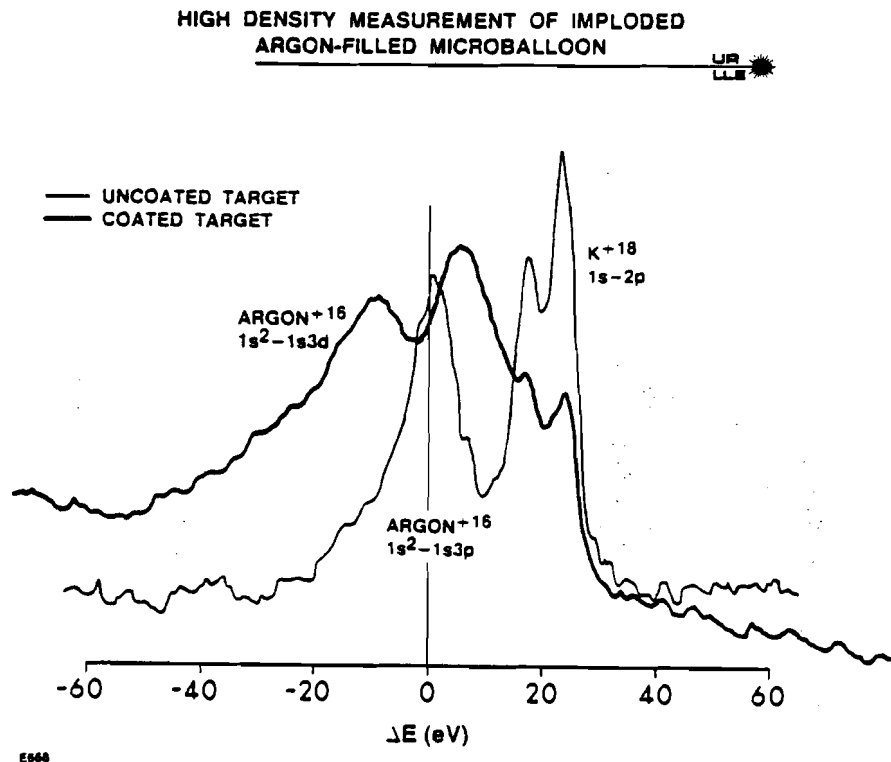
Figure 15 Argon lines from shot 2495 (plastic coated target) and from shot 2416 (uncoated target)

HIGH DENSITY MEASUREMENT OF IMPLODED
ARGON-FILLED MICROBALLOON
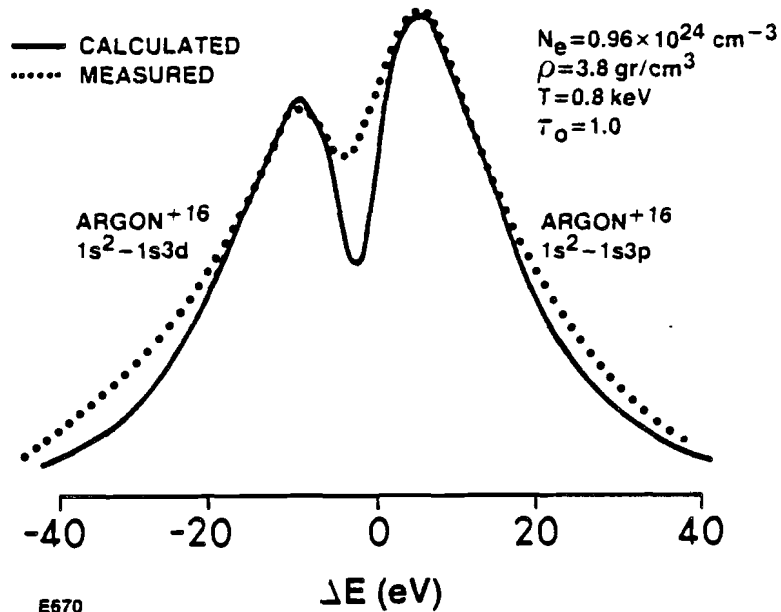
Figure 16 Density determination by fitting the observed lines for
shot 2495 in Figure 15 with a computed Stark profile

Analysis of Ar line profiles has yielded convincing evidence of compressed Argon densities in the range of 4-6 g/cm^3 (n_e = 1.0 - 1.5 x 10^{24} cm^{-3}). Analysis of the optically thick Ar^{+17} Lyman-α line also yields information on the Argon ρR at time of emission: for example, for shot 3231, we find ρR = 1.5 ± 0.5 x 10^{-3} g/cm^2. The ρ and ρR determinations are consistant with each other if the Ar is assumed to be totally confined inside the tamping shell. We therefore have additional evidence that for the symmetrical illumination of the ZETA laser system, the implosion symmetry is good and significant shell breakup does not occur (up too the time of line emission).

The relatively high density obtained with these Argon filled targets is due in part to radiational cooling of the Argon. This can be seen from LILAC simulations for these experiments. Figure 17 shows the average temperature and density time histories in the Argon for a thick shell Argon filled target. The cooling immediately following the temperature maximum is due largely to Argon radiational cooling, and significantly increased densities result. The simulations are done with a rate equation treatment for the Argon ionization states, and show that the line emission occurs in a short ($\sim$ 10 psec) time interval around the time indicated. This explains why the experimental profiles can be so well fit by a theoretical profile for a single density. The Argon line profiles produced in the simulation also match well with experimental profiles.

ARGON TIME HISTORY

Ly β Emission from
Rate Equations

T_e

ρ

T_e (eV)

ρ (g / cc)

SiO$_2$ 2.9 μ

Argon
7 atm   31 μ

0.3 TW absorbed
65 psec

TIME (psec)
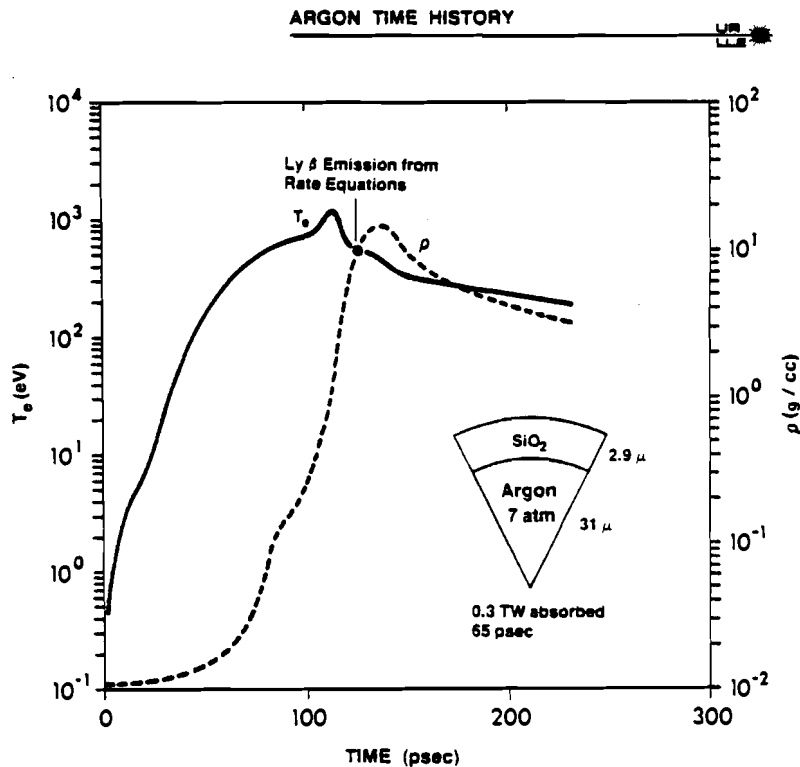
TC541

Figure 17   Average temperature and density time histories calculated by LILAC

1. B. Yaakobi, S. Skupsky, R. L. McCrory, C. F. Hooper, Jr.,
    H. Deckman, P. Bourke, and J. M. Soures, "Symmetric Laser
    Compression of Argon-Filled Shells to Densities of 4-6 g/cm^3,"
    submitted to Physical Review Letters.

Diagnostic Development: Alpha Particle Imaging

Successful fabrication of free standing gold zone plates of up to 8 μm thickness has been accomplished. This has enabled the recording of alpha-particle coded images on a few high yield exploding pusher implosions on ZETA. First order reconstructed images have been obtained in two cases, one corresponding to symmetrical focusing and implosion, and the other to center focusing conditions. Figure 18 shows isodensity contours obtained from the reconstruction for the two shots. They correspond to contours of constant alpha-particle time-integrated intensity, which displays a peak in the center for both shots. The targets had diameters of 112 μm, wall thicknesses of 0.7 μm, and were filled with 20 atm of DT. For Figure 18a, the beams were focused for near symmetrical illumination and the alpha-particle contours are roughly circular extending over a region about 30 μm in diameter. The yield for this shot was 1.1×10^9 with 1.8 TW on target. For Figure 18b, the beams were focused on the center of the target, which resulted in significant structure in the x-ray image. Similarly, the alpha-particle contour plot shows evidence of the six ZETA beams. A reduced yield of 4.7×10^8 was obtained with 2.05 TW on target. We have tentatively concluded that the outward extensions of the contours in Figure 18b are along the incident beam directions.

(a)

|←———30 μm———→|

|←——————————Initial Target Diameter——————————→|
112 μm

(b)

|←————50 μm————→|
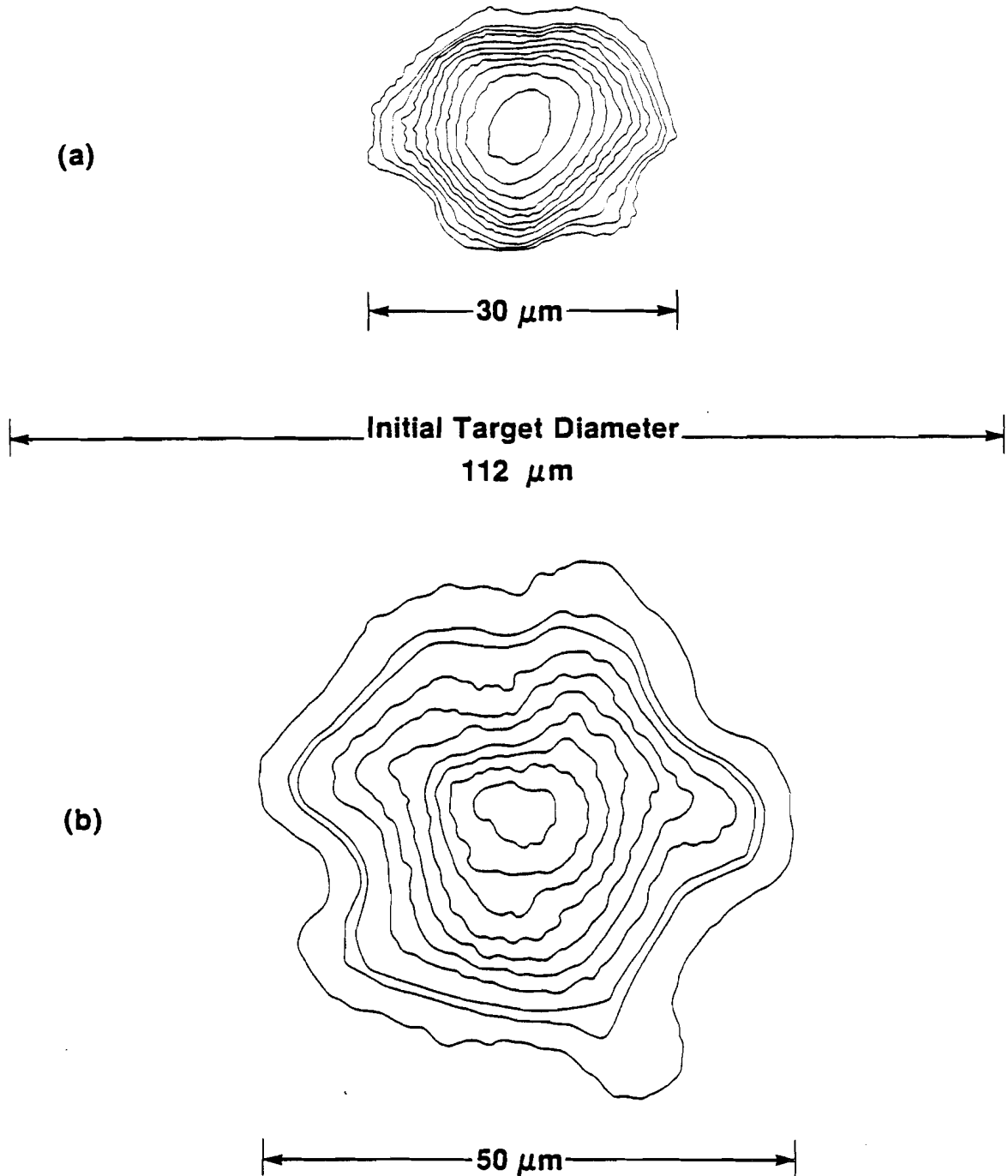
Figure 18   Contours of constant alpha-particle time-integrated
intensity: (a) beams focused 1.4 radii beyond the
target center for near symmetrical illumination;
(b) beams focused at the target center

OMEGA BOOSTER PROGRAM

The feasibility program for upgrading OMEGA laser power through addition of active mirror amplifiers has continued during the past quarter. The booster scheme being considered for OMEGA would consist of 4-6 active mirror amplifiers at the end of each beam line to increase laser power by about a factor of 4. During the last quarter, the construction of a prototype 21 cm active mirror amplifier was completed; the previous experimental version was 17 cm in diameter. A 500 shot life test was performed with the flashlamps firing to determine the reliability of the new components. No major problems were uncovered with the new design. We did find, however, that the latest batch of AR treated pyrex used in the lamp jackets and blast shields did begin to show damage from the flashlamp light. We are currently working with Corning Glass to track down the cause of this new problem. The cooling time (i.e., time to reach thermal equilibrium) for the 21 cm active mirror was measured to be 18 minutes. This is consistent with the OMEGA shot cycle of 30 minutes. The small signal gain of the active mirror without a front face coating was measured to be 1.52 corresponding to a stored energy density of .329 J/cm^3. When the front face coating is added the gain is increased to 1.59 and the stored energy density becomes .365 J/cm^3. These results are in good agreement with the prediction of Active Mirror simulation code INVDEN.

ADVANCES IN TARGET FABRICATION

A Drill and Plug Technique for Filling Laser Fusion Targets

A new technique has been developed for filling hollow glass shell (microballoon) laser fusion targets with gases. Each microballoon is filled through a laser-drilled micron or submicron sized hole which is sealed using a single glass or plastic plug of comparable dimension. The seal is formed by melting a plug that was transferred onto the hole prior to filling. This technique was designed primarily to fill microballoons with Ar and other gases having low permeability through glass. The Ar targets for the intermediate density implosion experiments described on pages 25-30 were filled with this method.

Holes are drilled using 80 psec laser pulses of wavelength 1.06μm. It has been found possible to produce high aspect ratio holes smaller than the diffraction limited laser spot size. Aspect ratios as high as 3:1 have been obtained, although typically the laser is configured to produce an aspect ratio of 1:1 which yields 0.5 - 2.5 μm holes in the microballoons of interest.

Plug materials which have been used to seal holes include 1-5 μm diameter polystyrene spheres and irregularly shaped pieces of low melting point glass of ~ 2 μm dimension. Since the plug is chosen from a material which can later be melted to form the seal, each plug can be transferred onto the hole at ambient atmospheric conditions.

Plugs are usually melted after the microballoons have been pressurized and flow in a manner such that the perturbation to the surface finish can be as small as 2000 $\overset{o}{A}$ with a width of 2-4 μm. Figure 19 shows the surface of a microballoon which has been filled with 30 atm of Ar and sealed by melting a polystyrene sphere over the filling hole.

To certify the integrity of the seal, the optical path length through the balloon is interferometrically measured before and after filling. The change in optical path length is a direct measure of the gas pressure trapped inside a balloon. As expected, the pressure retention half life is dependent upon the interior volume of the balloon as well as the specific gas being trapped. For Ar trapped inside a 60 μm diameter microballoon, the pressure retention half-life is 12-30 hours when a polystyrene plug is used and well in excess of a month when sealed with a glass plug.

AN ARGON-FILLED MICROBALLOON PREPARED BY THE DRILL AND PLUG TECHNIQUE
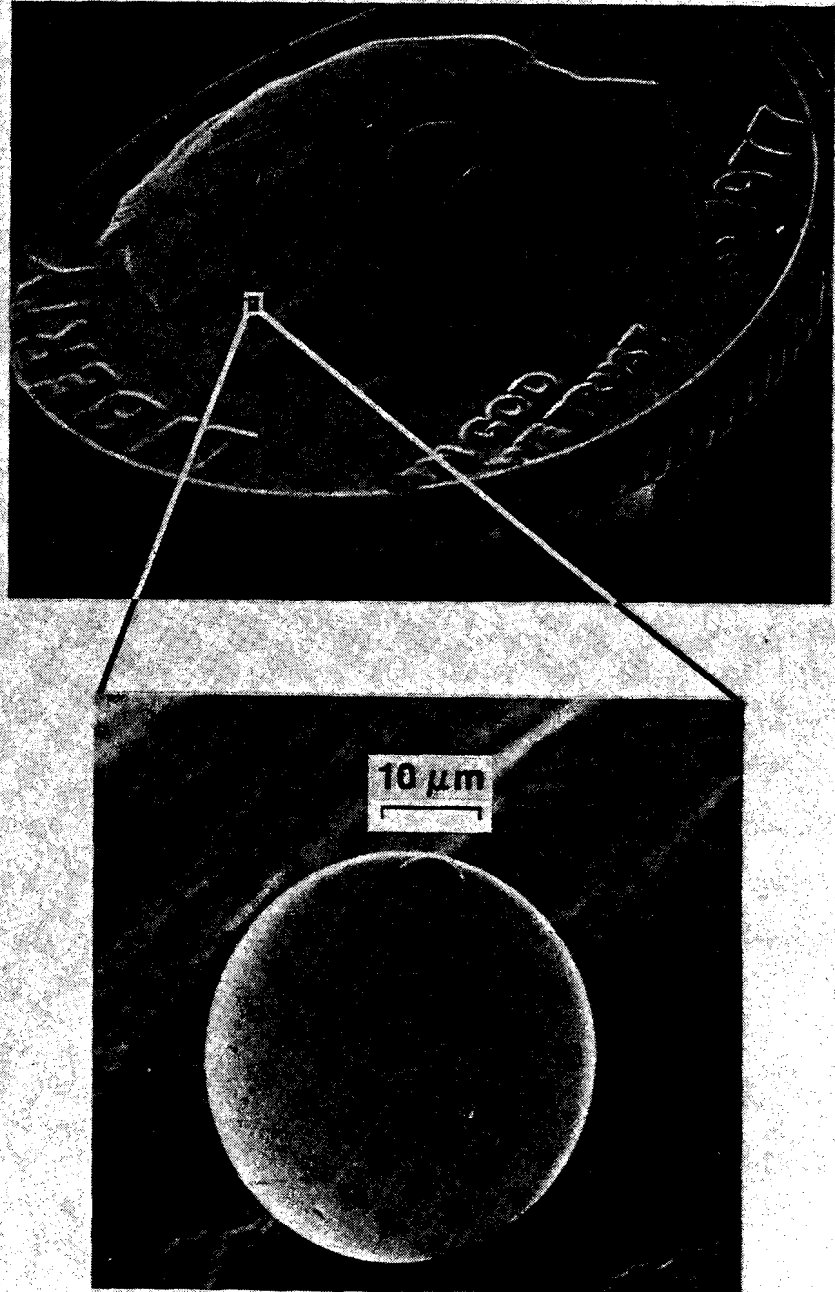
Figure 19

Self-Consistent, Non Destructive Measurement of Tritium Content and
Wall Thickness of Glass Microballoon Laser Fusion Targets

In laser fusion experiments employing gas filled microballoons, it
is essential that the fill pressure and glass wall thickness be known
for each target prior to its use. While most targets retain their
original fill pressure "indefinitely" when stored at liquid nitrogen
temperature, some leakage has been found to occur in random samples.
Previously, we have reported[1] a method for determining the tritium
content of microballoon targets by measuring the flux of beta particles
from the decay of tritium which emerge from the target wall. Since it
was found that tritium and deuterium leak from glass microballoons at
the same rate, a measurement of only the tritium content is sufficient
to completely characterize the target fill. In order to relate beta
particle count to tritium pressure, an accurate knowledge of the shell
wall thickness is required. Optical interference methods[2,3] are useful
for wall measurements; however, corrections must be applied to account
for the optical path length contributions from the gas within the
target. Furthermore, the measured beta flux is reduced due to
interactions with the fill gas; and a significant correction is
required for high pressures and large microballoon diameters.

Because the wall thickness and pressure measurements are
interdependent, an iterative technique has been developed to determine
self-consistent parameters from the basic experimental input data.
Required in the analysis, which relates measured beta flux to tritium
fill pressure, is a quantitative modeling of the transmission of the

betas through the fill gas and glass walls. This model was developed using the Monte Carlo code, SANDYL, which calculates the net transmission probability for betas created uniformly within a spherical microsphere with the appropriate distribution of initial energies. Each code run follows the trajectories of 100,000 betas which are initially distributed according to the well-known energy spectrum of tritium beta decay. The particles are transported through the gas fill region and the glass wall accounting for such physical processes as slowing down due to inelastic collisions and the tracking of secondary electrons.

In the present application, the sample trajectories are used to calculate the fraction of source particles which emerge from the target as a function of total gas pressure p (atm), microballoon outer diameter D (μm) and wall thickness t (μm). For equi-molar deuterium-tritium fills and glass walls (density = 2.5 g/cm^3) the transmitted fraction is accurately represented by the expression: $f = 1.007 \exp(-2.717 \times 10^{-5} p D) \exp(-2.769 t)$ for $0 < p < 100$ atm, $50 < D < 200$ μm and $.4 < t < 2$ μm. This expression agrees well with previous estimates[1,4] of the transmission fraction.

Using an assumed pressure p_0 (e.g., the permeation pressure), a wall thickness t_0 is calculated from: $t_0 = x\lambda - 1.30 \times 10^{-4} p_0 D$; where x is the measured fringe shift. This expression includes a correction for the refractive index of deuterium and tritium based upon the estimates of Briggs et. al.[5]. Using t_0 and the measured beta count rate C, a corrected pressure p_1 is calculated using the method of Reference 1. This new value of p_1 is then used to calculate a

corrected thickness t_1. Typically 6-8 iterations yield convergence in p and t to 5% or better.

This technique has proven quite useful in providing a self-consistent measurement of the pressure content and wall thickness of deuterium- tritium filled glass microballoons.

1. H. W. Deckman, G. M. Halpern, J. Appl. Phys. <u>50</u>, 132 (1979).

2. B. W. Weinstein, J. Appl. Phys. <u>46</u>, 5305 (1975).

3. G. M. Halpern, J. Varon, D. C. Leiner, D. T. Moore, J. Appl. Phys. <u>48</u>, 1223 (1977).

4. M. Mueller, Los Alamos Laboratories (private communication).

5. C. K. Briggs, R. T. Tsugawa, C. D. Hendricks, P.C. Souers, UCRL-51921.

Improvements in Parylene Coating of Fusion Targets by Molecular Structure Changes

Deposition of polymer coatings on glass microballoons is a convenient method for obtaining thick shell targets for laser fusion experiments. Since surface perturbations in the coating will cause the symmetry of the implosion to deteriorate, it is essential to be able to place extremely uniform polymer coatings onto the surface of a target, preferably at fast deposition rates. We have found that uniform plastic coatings can be made by using the Parylene process[1] of Union Carbide if molecular structure changes are made to the commercial material Parylene N (Poly (p-xylylene)). These coatings are applied without special cooling or heating arrangements, i.e., at 25 ^{o}C.

Problems with Parlalene N coatings were noted by Liepins et. al.[2] Unacceptable surface finish is obtained with too high a deposition rate, while slow rates of deposition produce surfaces relatively free of non- uniformities. This is due to the fact that the polymer coating typically has a high degree of crystallinity (60%) and is therefore quite susceptable to nucleation on a highly nucleating surface such as glass. On a very clean surface at room temperture, the deposition rate of parylene N is about 0.5 µm/hour in order to obtain an acceptable surface finish. If the surface were not clean, the deposition rate would have to be even lower. This is illustrated in Figure 20(a), which shows the surface finish of a parylene N(Poly(p-xylylene)) coating applied to an uncleaned surface at 1 µm/hour. The regular molecular structure (shown to the right) leads to

(a)

Poly (p-xylylene)

10 μm

(b)

Poly (ethyl-p-xylylene)
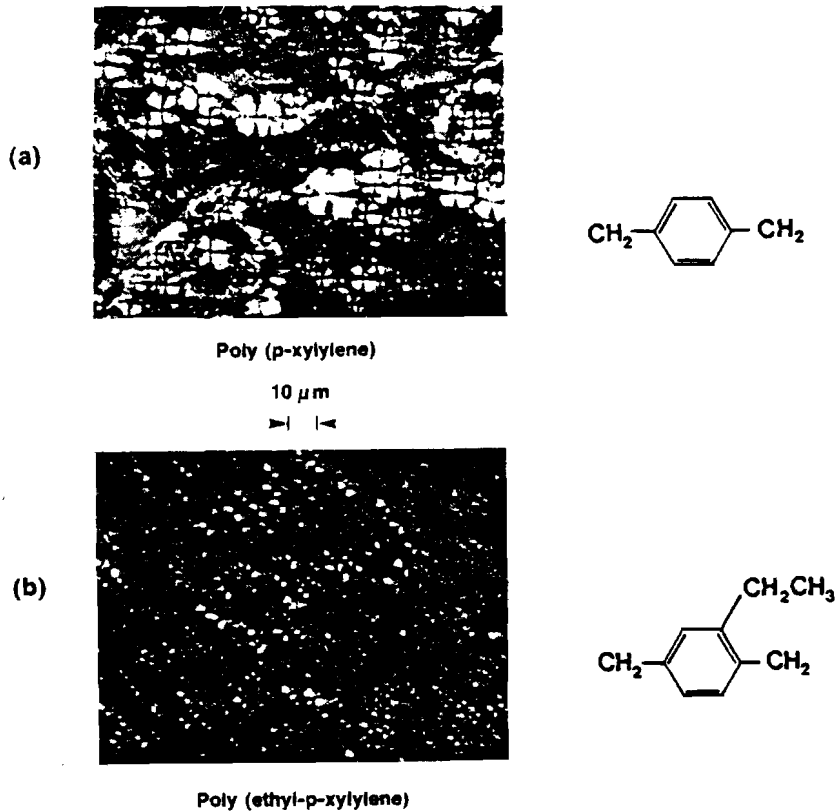
Figure 20 Improvements in surface finish and deposition rate for Parylene coated targets is obtained by making molecular structure changes to Parylene N: (a) surface finish for Parylene N; (b) surface finish with modified structure

the growth of crystalline formations and an unacceptable surface finish results. It has been found that by modifying the molecular structure of parylene N as shown in Figure 20(b), the tendency to nucleate is much reduced. The coating in Figure 20(b) was also applied to an uncleaned surface but at 2 μm/hour. With appropriately prepared surfaces, target quality coatings (structure size ≤ 0.1 μm) are obtained at 2 μm/hour deposition rates with Poly(ethyl-p-xylyene).

1. W. F. Gorham, J. Polymer Sci., A-1, $\underline{4}$ 3027 (1966).

2. R. Liepins, M. Campbell, and R. J. Fries, ACS Polymer Preprints (Organic Coating and Plastic Chem.),Vol. $\underline{40}$, 175 (1979).

National Laser Users Facility News

On November 29 and 30, a workshop was held at LLE to consider possible laser experiments in areas outside laser fusion. Over fifty scientists attended, chosen for their expertise in disciplines unconnected with laser fusion, but which nevertheless could benefit from experiments using high power lasers. It was the consensus of those attending the workshop that the major impact in biology and chemistry will be through EXAFS (Extended X-ray Absorption Fine Structure) studies or x-ray diffraction techniques. Development of the latter is underway at LLE and steps are being taken to improve the resolution to the level necessary. Equation of state studies can be extended to new regions through the extremely high velocity shock waves that can be driven by high power lasers. Damage effects created by lasers in a variety of materials are of interest to workers in material properties. The high neutron flux generated during implosion experiments could be of interest due to the effect produced in materials, but this subject needs further investigation. There are a variety of applications in general physics, including the study of highly ionized atoms, cross-section measurements at relatively low energies using laser — produced ions and multiphoton ionization processes.

A report on the workshop is being prepared and will be available shortly.

LLE FACILITY REPORT

In November, 1979, our CDC 6600 Computer System was upgraded to a CDC CYBER 175 System resulting in a 50% increase in memory and a 2 to 5 fold increase in central processor speed.

PUBLICATIONS AND CONFERENCE PRESENTATIONS

PUBLICATIONS

"Six Beam Irradiation and Implosion of Laser Fusion Targets: Laser Fusion Targets: Laser Focus Dependence," E. I. Thorsos, T. C. Bristow, J. A. Delettrez, J. M. Soures, and J. Rizzo; Appl. Phys. Lett. 35, 598 (1979).

"Search for Shell Disintegration in Laser Implosion Experiments," K. Tanaka and E. I. Thorsos; Appl. Phys. Lett. 35, 853 (1979).

"Active Pulse Shaping in the Picosecond Domain," J. Agostinelli, G. Mourou and C. Gabel; Appl. Phys. Lett. 35, 731 (1979).

"High Power Switching with Picosecond Precision," G. Mourou and W. Knox; Appl. Phys. Lett. 35, 492 (1979).

"Optical Pulse Shaping with a Grating Pair," J. Agostinelli, G. Harvey, T. Stone and C. Gabel; Appl. Optics 18, 2500 (1979).

"Explosive-Pusher-Type Laser Compression Experiments with Neon-Filled Microballoons," T. C. Bristow, J. Delettrez, A. Entenberg, Y. Gazit, A. Hauer, L. Goldman, E. Lazarus, C. Lee, S. Letzring, M. Lubin, R. McCrory, T. Mukaiyama, B. Nicholson, B. Perry, J. Rizzo, S. Skupsky, J. Soures, D. Steel, E. Thorsos, and B. Yaakobi; Plasma Physics and Controlled Nuclear Fusion Research (International Atomic Energy Agency, Vienna, 1979), Vol. III, p. 29.

PAPERS SUBMITTED FOR PUBLICATION

"Spectral Methods for Multi-Dimensional Diffusion Problems," R. L. McCrory and S. A. Orszag (to be published in J. Comp. Physics).

"Dense Matter in Laser Fusion Experiments," R. L. McCrory and J. Wilson (to be published in l'Edition Francaise Physique, E. Shatzman, Ed.).

"X-Ray Line Shift as a High-Density Diagnostic for Laser Imploded Plasmas," S. Skupsky (to be published in Phys. Rev. A).

"Fast Ion Production by Suprathermal Electrons in Laser Fusion Plasmas," M. A. True, J. R. Albritton and E. A. Williams (submitted to Physics of Fluids).

"Measurements of Brillouin Backscatter Dependence on Density Scale Lengths Near Critical Density," R. E. Turner and L. M. Goldman (submitted to Physical Review Letters).

"Evidence for Multiple Brillouin Modes in Laser-Plasma Backscatter Experiments," R. E. Turner and L. M. Goldman (submitted to Physical Review Letters).

"Design and Performance Characteristics of a High Power Phosphate Glass Laser System," W. Seka, J. Soures, O. Lewis, J. Bunkenburg, D. Brown, S. Jacobs, G. Mourou, and J. Zimmerman (submitted to Applied Optics).

"Picosecond Switching of a Multi-kilovolt DC Bias with Laser Activated Silicon at Low Temperature," M. Stavola, M. G. Sceats, and G. Mourou (submitted to Applied Physics).

CONFERENCE PRESENTATIONS

I. American Physical Society - Division of Plasma Physics, Boston, November 12-16, 1979.

"Implosion of Argon-Filled Glass Microballoons with the ZETA Laser System," B. Yaakobi, T. C. Bristow, S. Skupsky, R. L. McCrory, P. Bourke, H. Deckman, and J. Soures.

"Determination of Time-Varying Electrostatic Potentials in Laser Fusion Targets from Alpha Particle Spectra," J. Delettrez, Y. Gazit, A. Entenberg, and J. Virmont.

"Effect of Electric Field on Charged Reaction Product Spectra in 6-Beam Symmetrical Implosion Experiments," Y. Gazit, J. Delettrez, A. Entenberg, T. C. Bristow, and J. Soures.

"Absorption Measurements for Glass Microballoon Implosions with 6-Beam Irradiations at 1.06µ," W. Seka, R. Hutchison, and R. Nimick.

"Brillouin Backscatter Dependence on Density Scale Lengths Near Critical Density," R. E. Turner and L. M. Goldman.

"Intensity and Time Calibration of a Picosecond X-Ray Streak Camera with Accurate Time Fiducials," W. D. Friedman, S. A. Letzring, J. E. Rizzo, and W. Seka.

"Search for Shell Disintegration in Laser Implosion Experiments," K. Tanaka and E. I. Thorsos.

"Measurements of the Dynamics of Exploding Pusher Targets," S. A. Letzring and M. Lubin.

"Symmetrical Implosion Experiments - Results with Exploding Pusher Targets," T. C. Bristow, J. Delettrez, A. Entenberg, W. Friedman, Y. Gazit, S. Letzring, W. Seka, J. Soures, E. Thorsos, and B. Yaakobi.

"Implosions with Plastic Coated Glass Microballoons on ZETA," E. I. Thorsos, W. Seka, T. Bristow, J. Delettrez, A. Entenberg, W. Friedman, R. McCrory, J. Rizzo, J. Soures, and B. Yaakobi.

"Symmetrical Illumination Laser Fusion Implosion Experiments at the University of Rochester's National Laser User Facility," J. M. Soures (invited paper).

"Focusing X-Ray Spectrograph for Laser Fusion Experiments," B. Yaakobi, R. E. Turner, P. Bourke, and J. Soures.

"Nonlinear Development of Ablation Driven Rayleigh-Taylor Instability," R. L. McCrory, R. L. Morse, and C. P. Verdon.

"Two Dimensional Lagrangian Modeling and Unstable Hydrodynamic Flows," C. P. Verdon, R. L. McCrory, R. L. Morse.

"Ion Current Measurement as a Diagnostic of Laser Imploded Spherical Shells," B. Nicholson, J. Delettrez, B. Yaakobi, and M. Lubin.

"Simulation of Fast Ion Generation in Laser Driven Implosions," J. Virmont and J. Delettrez.

"Theoretical Simulation of High Density Experiments at the University of Rochester," S. Skupsky, R. L. McCrory, and B. Yaakobi.

"Spectral Methods for Multi-Dimensional Diffusion Problems," S. A. Orszag and R. L. McCrory.

"Implosion Dynamics of Asymmetrically Illuminated Radiationally Cooled Targets for ZETA," R. S. Craxton and R. L. McCrory.

II. Optical Society of America, Annual Meeting, Rochester, New York, October 1979.

"Laser Drilling with 80 psec Pulse Lengths," H. W. Deckman, J. Drumheller, and J. Rizzo.

"Microdensitometer Using Backscattered Electrons," H. W. Deckman and D. Black.

"Monochromatic Soft X-Ray Source for Contact Microradiography," H. W. Deckman and J. H. Dunsmuir.

"Picosecond Active Pulse Shaping," J. Agostinelli, G. Mourou and C. W. Gabel.

"Normal-Incidence Soft X-Ray Reflectors for Arbitrary Wavelengths Using a Modified Langmuir-Blodgett Method," A. E. Rosenbluth and J. M. Forsyth.

"Extreme-Ultraviolet and X-Ray Spectroscopy of an Inverted Laser-Produced Aluminum Plasma," Yves Conturie and J. M. Forsyth.

"Contributions to Information and Noise in Zone-Plate Coded Imaging from Various Recording Media," F. D. Kalk and J. M. Forsyth.

"X-Ray Diagnostics in Laser-Fusion Experiments," J. M. Forsyth (invited paper).

III. Other Meetings

"Switching with Picosecond Precision with Laser Activated Semiconductor Switches," G. Mourou; invited paper presented at the 3rd Annual IEEE Conference on Electronic Device Activities in Western New York, October 18, 1979.

"Nanosecond X-Ray Diffraction of Biological Samples Using a Laser Plasma Source," J. Forsyth; invited paper presented at New York State Section Meeting of the American Physical Society, October 1979.

"High Power Glass Lasers and Their Application to Controlled Thermonuclear Fusion," invited paper presented by J. Soures at the New York State Section Meeting of the American Physical Society, October 1979.

"High Density Compression Experiments at LLE," presented by J. Soures at the Fifth Workshop on Laser Interaction with Matter, November 1979.

"Dense Matter in Laser Fusion: Experiments," R. McCrory and J. Wilson, Colloquium of High Density Matter, September 1979.

"Electronic, Nuclear, and Total Nonlinear Indices of Liquids," D. C. Brown, J. M. Rinefierd, S. D. Jacobs, and J. A. Abate; Eleventh Annual Symposium on Optical Materials for High Power Lasers, Boulder, Colorado, October 30-31, 1979.